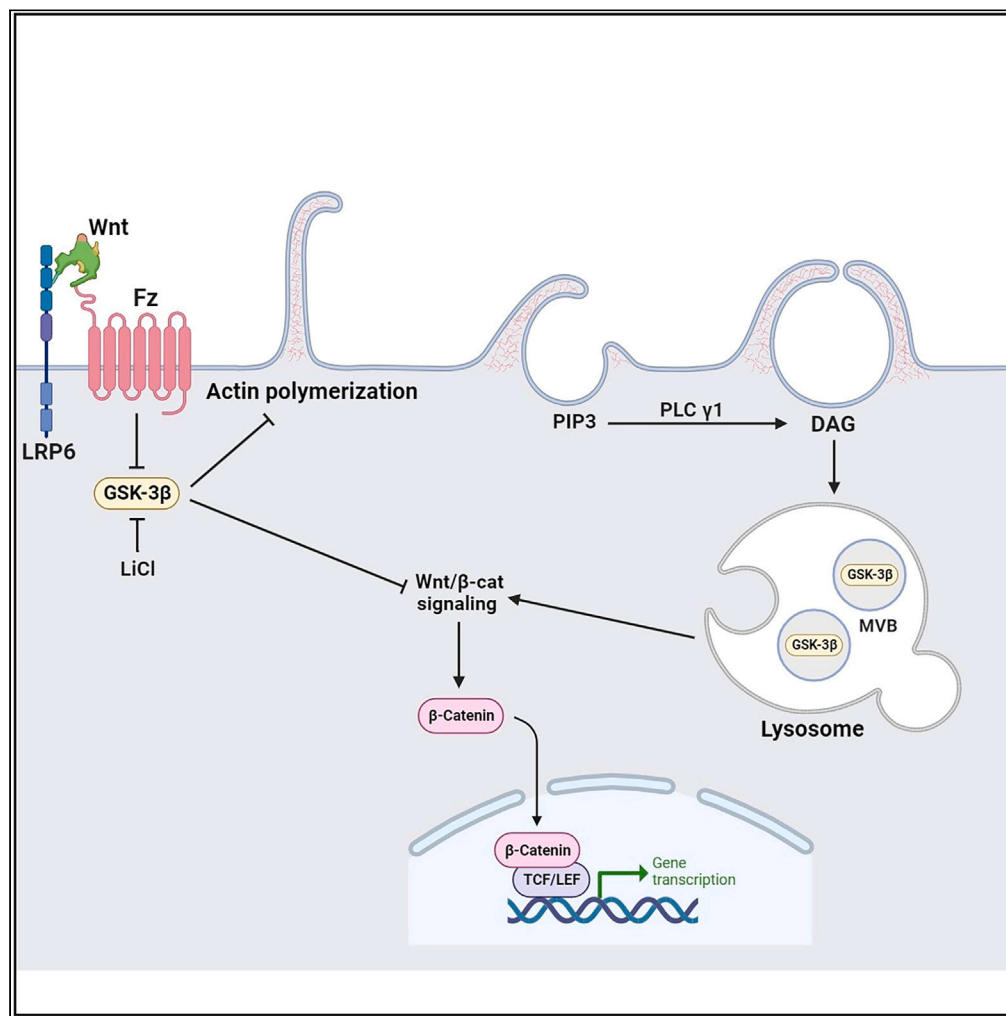


## Article

Addition of exogenous diacylglycerol enhances Wnt/ $\beta$ -catenin signaling through stimulation of macropinocytosis

Yagmur Azbazdar,  
Nydia Tejada-  
Munoz, Julia C.  
Monka, Alex  
Dayrit, Grace  
Binder, Gunes  
Ozhan, Edward M.  
De Robertis

ederobertis@mednet.ucla.edu

**Highlights**

Addition of the lipid diacylglycerol triggers macropinocytosis in cultured cells

DAG signaling enhances Wnt signaling through macropinocytosis

The multivesicular body marker CD63 is increased by DAG

DAG synergizes with LiCl inducing ectopic neural axes in *Xenopus*

Azbazdar et al., iScience 26,  
108075  
October 20, 2023 © 2023 The  
Author(s).  
[https://doi.org/10.1016/  
j.isci.2023.108075](https://doi.org/10.1016/j.isci.2023.108075)

## Article

Addition of exogenous diacylglycerol enhances Wnt/ $\beta$ -catenin signaling through stimulation of macropinocytosis

Yagmur Azbazzdar,<sup>1,5</sup> Nydia Tejada-Munoz,<sup>1,2,5</sup> Julia C. Monka,<sup>1</sup> Alex Dayrit,<sup>1</sup> Grace Binder,<sup>1</sup> Gunes Ozhan,<sup>3,4</sup> and Edward M. De Robertis<sup>1,6,\*</sup>

## SUMMARY

**Activation of Wnt signaling triggers macropinocytosis and drives many tumors. We now report that the exogenous addition of the second messenger lipid sn-1,2 DAG to the culture medium rapidly induces macropinocytosis. This is accompanied by potentiation of the effects of added Wnt3a recombinant protein or the glycogen synthase kinase 3 (GSK3) inhibitor lithium chloride (LiCl, which mimics Wnt signaling) in luciferase transcriptional reporter assays. In a colorectal carcinoma cell line in which mutation of adenomatous polyposis coli (APC) causes constitutive Wnt signaling, DAG addition increased levels of nuclear  $\beta$ -catenin, and this increase was partially inhibited by an inhibitor of macropinocytosis. DAG also expanded multivesicular bodies marked by the tetraspan protein CD63. In an *in vivo* situation, microinjection of DAG induced Wnt-like twinned body axes when co-injected with small amounts of LiCl into *Xenopus* embryos. These results suggest that the DAG second messenger plays a role in Wnt-driven cancer progression.**

## INTRODUCTION

Plasma membrane lipid-derived signals such as phosphatidylinositol-3,4,5-triphosphate (PIP3) and diacylglycerol (DAG) are major regulators of cellular responses to extracellular signaling in physiology and cancer progression.<sup>1–3</sup> Wnt canonical signaling is also a major regulator of carcinogenesis.<sup>4</sup> How mutations in these oncogenic pathways crosstalk to each other is an important problem in the integration of cell signaling. In addition, it has long been known that cancer progression is also influenced by substances that do not mutate the DNA by themselves but facilitate cancer development, which are called tumor promoters.<sup>5–7</sup> The prototype tumor promoter is the phorbol ester phorbol-12-myristate-13-acetate (PMA), which mimics the second messenger DAG on the plasma membrane. DAG is an activator of the protein kinase C (PKC) signaling pathway.<sup>8–10</sup> We now show that direct addition of DAG dissolved in dimethyl sulfoxide (DMSO) strongly potentiates macropinocytosis and Wnt signaling.

Wnt growth factors bind to their surface membrane receptors Frizzled (Fz) and low-density lipoprotein receptor-related protein 6 (LRP6), resulting in the stabilization of  $\beta$ -catenin. In the absence of Wnt,  $\beta$ -catenin is degraded by a cytosolic destruction complex containing adenomatous polyposis coli (APC), Axin1, casein kinase 1 (CK1), and the key regulator glycogen synthase kinase 3 (GSK3). This destruction complex is inactivated by Wnt signaling.<sup>11,12</sup> Activation of the Wnt pathway is a major driver of cancer.<sup>13,14</sup> For example, colorectal carcinoma (CRC) and hepatocellular carcinoma (HCC) frequently carry loss-of-function mutations in the degradation complex components APC or Axin1, resulting in constitutive  $\beta$ -catenin signaling.<sup>15–18</sup>

Recent work has shown that in the presence of Wnt, receptor complexes are endocytosed and translocated into the intraluminal vesicles of multivesicular bodies (MVBs).<sup>19,20</sup> Activated Wnt receptors bind components of the destruction complex such as GSK3 and Axin1, which are endocytosed together with them. The formation of MVBs is part of the normal membrane trafficking machinery, and all plasma membrane proteins must transit through MVBs/late endosomes to reach lysosomes for degradation. Thus, the Wnt signaling pathway co-opted normal cellular trafficking to achieve the regulated sequestration of GSK3 and Axin1 from the cytosol.<sup>20</sup>

Macropinocytosis (Greek, *pinein*, to drink) is an actin-mediated cell drinking process that involves the uptake of large fluid vesicles carrying extracellular nutrients into endocytic cups that are several microns in diameter.<sup>21–23</sup> A number of signaling pathways, such as EGFR and other receptor tyrosine kinases, can transiently induce macropinocytosis<sup>24</sup> through to the activation of phosphoinositide 3 kinase (PI3K) and the

<sup>1</sup>Department of Biological Chemistry, David Geffen School of Medicine, University of California Los Angeles, Los Angeles, CA 90095-1662, USA

<sup>2</sup>Department of Oncology Science, Health Stephenson Cancer Center, University of Oklahoma Health Science Center, Oklahoma City, OK 73104, USA

<sup>3</sup>Department of Molecular Biology and Genetics, Izmir Institute of Technology, Urla, Izmir 35430, Türkiye

<sup>4</sup>Izmir Biomedicine and Genome Center (IBG), Dokuz Eylul University Health Campus, Inciralti-Balcova, Izmir 35340, Türkiye

<sup>5</sup>These authors contributed equally

<sup>6</sup>Lead contact

\*Correspondence: [ederobertis@mednet.ucla.edu](mailto:ederobertis@mednet.ucla.edu)

<https://doi.org/10.1016/j.isci.2023.108075>



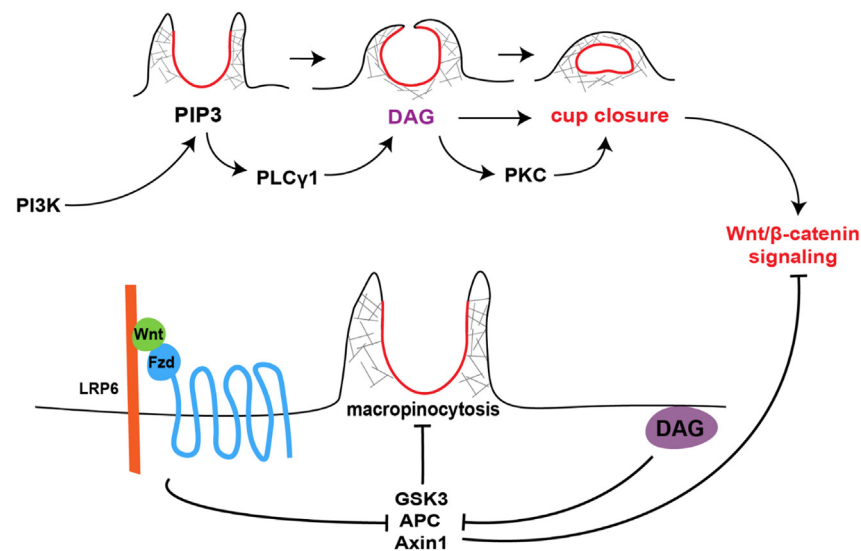


**Figure 1. Diagram of the regulation of macropinocytosis by PI3K, DAG, Wnt/β-catenin, GSK3, APC, and Axin1 from the literature and the present paper**

PI3K activated by RTKs or G-protein coupled receptors leads to the generation of PIP3 in the plasma membrane, which triggers the formation of macropinocytotic cups by the actin cytoskeletal machinery network. PIP3 activates PLCγ and is itself converted into DAG, which in turn activates PKC which is required for cup closure and completion of macropinocytosis.<sup>26</sup> In the lower part of the diagram, Wnt signaling, through its Frizzled (Fzd) and LRP6 receptors, inhibits a destruction complex containing GSK3, APC, and Axin1 by translocating it into MVBs. In the absence of Wnt, GSK3 normally suppresses macropinocytosis.<sup>29</sup> LiCl, used in this study, induces macropinocytosis by inhibiting GSK3. Exogenous DAG (purple oval) increases Wnt signaling by sequestration of the GSK3/APC/Axin1 destruction complex.

formation of patches of PIP3 in lamellipodia.<sup>25,26</sup> An important realization has been that canonical Wnt signaling triggers sustained macropinocytosis.<sup>27,28</sup> The endocytosed membrane containing Wnt receptor complexes is trafficked into MVBs and lysosomes which become more acidic.<sup>29</sup>

An unexpected role for the membrane lipid DAG in Wnt signaling has been uncovered by recent work involving plasma membrane lipidome profiles in HCC cell lines with or without the addition of Wnt.<sup>30</sup> It was found that Wnt3a conditioned medium significantly reduced DAG levels in isolated plasma membranes of three HCC cell lines with activating mutations in components of the Wnt pathway.<sup>30</sup> Although seldom used, DAG is able to activate PKC in intact cells.<sup>31</sup> The formation of macropinocytotic cups is driven by patches of PIP3 in the plasma membrane, and subsequently this lipid is converted into DAG through the action of phospholipase C gamma 1 (PLCγ1), a step required for macropinocytotic cup closure.<sup>26,32</sup> Importantly, it has long been known that PMA, which DAG would mimic, can stimulate macropinocytosis in macrophages, cells in which macropinocytosis is constitutive.<sup>33</sup>

In the present study, we investigated whether DAG addition stimulates macropinocytosis and Wnt signaling activity in mammalian cultured cell lines. We report that DAG rapidly induces macropinocytosis and potentiates nuclear β-catenin signaling. This occurs even in CRC cells mutant for APC that have elevated Wnt/β-catenin signaling. In an *in vivo* situation, DAG was able to induce Wnt-like twinned axes when co-injected with low amounts of the GSK3 inhibitor LiCl. The results presented here suggest a critical role for the second messenger DAG in the induction of cellular macropinocytosis and subsequent activation of the Wnt/β-catenin pathway.

## RESULTS

### DAG added to the culture medium stimulates macropinocytosis

Figure 1 summarizes in diagrammatic form current knowledge on macropinocytosis and the new findings reported here with respect to exogenous addition on DAG. Macropinocytosis is initiated by PIP3, which is then converted into DAG, a step required for cup closure.<sup>26,32</sup> Wnt signaling, through the inhibition of GSK3, induces actin polymerization and macropinocytosis activation. In the absence of Wnt, GSK3 activity represses macropinocytosis,<sup>29</sup> which is an ancestral endocytic function present constitutively in amebae and macrophages.<sup>23</sup> In the presence of Wnt, the destruction complex consisting of GSK3, APC, and Axin1 is inhibited by sequestration into MVB/lysosomes. Exogenous DAG (purple oval) promotes Wnt signaling by increasing macropinocytosis and GSK3 sequestration (see below).

In practical terms, macropinocytosis is currently defined by the uptake of tetramethyl rhodamine-dextran (TMR-dextran) 70 kDa, a dextran derivative with a hydrated diameter of >200 nm.<sup>34</sup> Endocytic vesicles of less than 100 nm are designated as micropinocytosis and do not incorporate TMR-dextran 70 kDa. As shown in Figures 2A–2C, sn-1,2 DAG added to the culture medium of HEK293 cells strongly stimulated TMR-dextran uptake after 1 h. Overnight incubation also resulted in smaller but numerous vesicles containing dextran (Figures 2D–2F). This experiment shows that exogenous DAG is a potent activator of macropinocytosis.

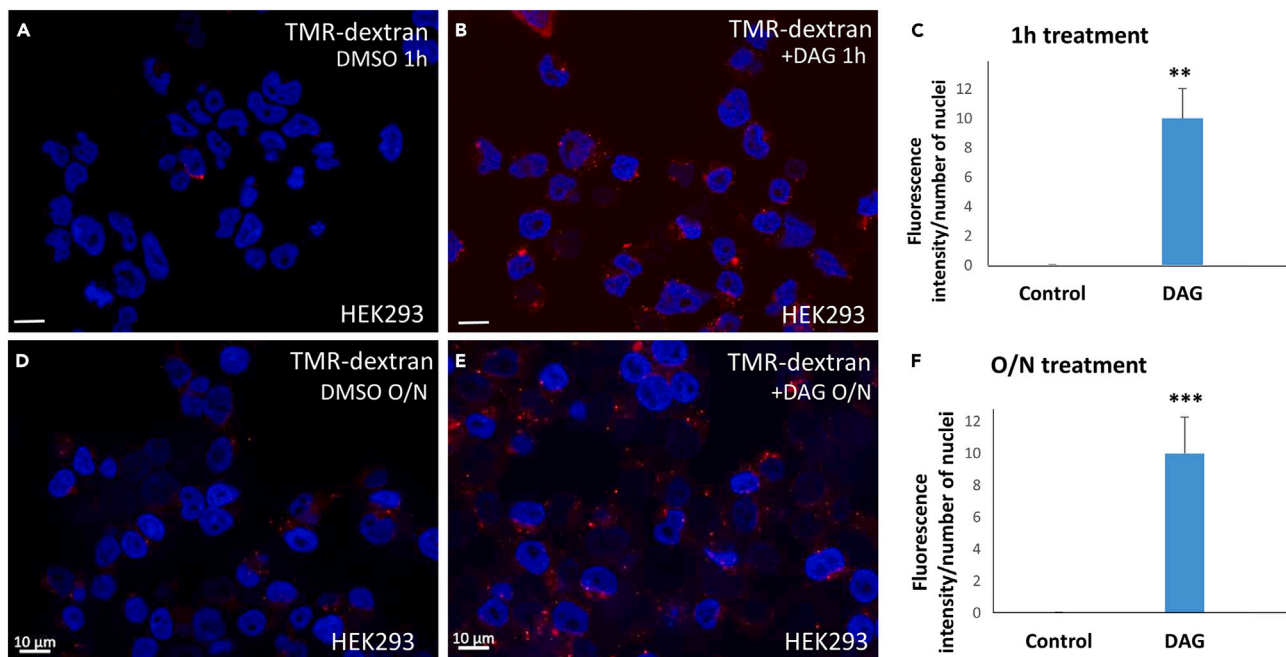


**Figure 2. Exogenous DAG added to the culture medium stimulates macropinocytosis in HEK293 cells**

(A and B) 35  $\mu$ M DAG, but not DMSO, increases the uptake of TMR-dextran 70 kDa, a marker of macropinocytosis after 1 h of addition.

(C) Quantification of TMR-dextran uptake after 1 h incubation with DAG using ImageJ.

(D and E) After overnight incubation, DAG treated cells contain small but numerous macropinocytotic vesicles.

(F) Quantification with ImageJ of TMR-dextran uptake after overnight incubation with DAG. Scale bars, 10  $\mu$ m; \*\* $p$  < 0.01 and \*\*\* $p$  < 0.001. Data are represented as mean  $\pm$  SD.

### DAG addition stimulates Wnt/ $\beta$ -catenin signaling

Next, we examined the effects of DAG on the activity of  $\beta$ -catenin activation reporter (BAR)<sup>35</sup> in a stably transfected HEK293 BAR-luciferase/Renilla cell line.<sup>28</sup> The addition of DAG to cells without any other treatment resulted in small but significant increases in  $\beta$ -catenin transcriptional signaling (Figure 3A). This increase is probably caused by low levels of endogenous Wnt signaling present in HEK293 cells, as reported previously.<sup>36</sup> In cells treated overnight with recombinant Wnt3a protein, DAG increased Wnt signaling activity (Figure 3B). LiCl is an inhibitor of GSK3 that mimics Wnt signaling and also triggers macropinocytosis.<sup>29</sup> In the presence of 40 mM LiCl, DAG potentiated Wnt/ $\beta$ -catenin signaling activity by 20-fold (Figure 3C). In the same HEK293 cells, addition of 35  $\mu$ M DAG for 2 h led to a strong stabilization of the tetraspanin protein CD63, a widely used marker of MVBs/lysosomes (compare Figures 3D–3G). The expansion of the MVB compartment is one of the downstream consequences of Wnt-induced macropinocytosis.<sup>37</sup> Interestingly, the key enzyme GSK3 tended to co-localize with CD63 (Figure 3I, arrows), and  $\beta$ -catenin protein localized to cytoplasmic vesicles (Figure S1) in HEK293 cells treated with DAG for 2 h. We conclude that exogenously added DAG promotes Wnt/ $\beta$ -catenin transcriptional signaling and this is accompanied by expansion of the MVB compartment.

### DAG increases nuclear $\beta$ -catenin in a CRC cell line mutant for APC in a macropinocytosis-dependent manner

We next asked whether DAG addition could further stimulate Wnt signaling in cancer cells in which the Wnt signaling pathway is constitutively activated by mutation of the tumor suppressor APC. SW480 is a CRC cell line that, despite decades in culture, can be reverted to a non-malignant phenotype by transducing full-length APC at endogenous expression levels.<sup>38,39</sup> SW480 cells have high nuclear  $\beta$ -catenin, and upregulated basal macropinocytosis and formation of MVBs/lysosomes.<sup>28</sup>

SW480 cells have elevated levels of nuclear  $\beta$ -catenin and detectable levels of the MVB/lysosome marker CD63 (Figures 4A–4C). Treatment with DAG (35  $\mu$ M) for 1 h greatly increased nuclear  $\beta$ -catenin as well as MVB levels (Figures 4D–4F). These effects were confirmed by western blot (Figure 4G). In cells transfected with myristoylated-GFP,<sup>40</sup> which marks the plasma membrane, DAG addition strongly increased macropinosome plasma membrane activity within minutes (Figure 4, compare panels H and I; Video S1). The increase in macropinosome number on the plasma membrane is observed almost immediately after addition of DAG (Video S2).

Remarkably, the effect of DAG on nuclear  $\beta$ -catenin was in addition to the constitutive stabilization caused by mutation of APC, which is the main oncogenic driver of this cancer cell line. Further, the expansion of MVBs positive for CD63 indicates that the DAG effect may be related to the stimulation of macropinocytosis. 5-N-ethyl-N-isopropyl amiloride (EIPA) is an inhibitor of macropinocytosis that acts by blocking the  $\text{Na}^+/\text{H}^+$  exchanger in the plasma membrane and inhibiting the actin machinery.<sup>41</sup> The uptake of TMR-dextran 70 kDa and its inhibition by

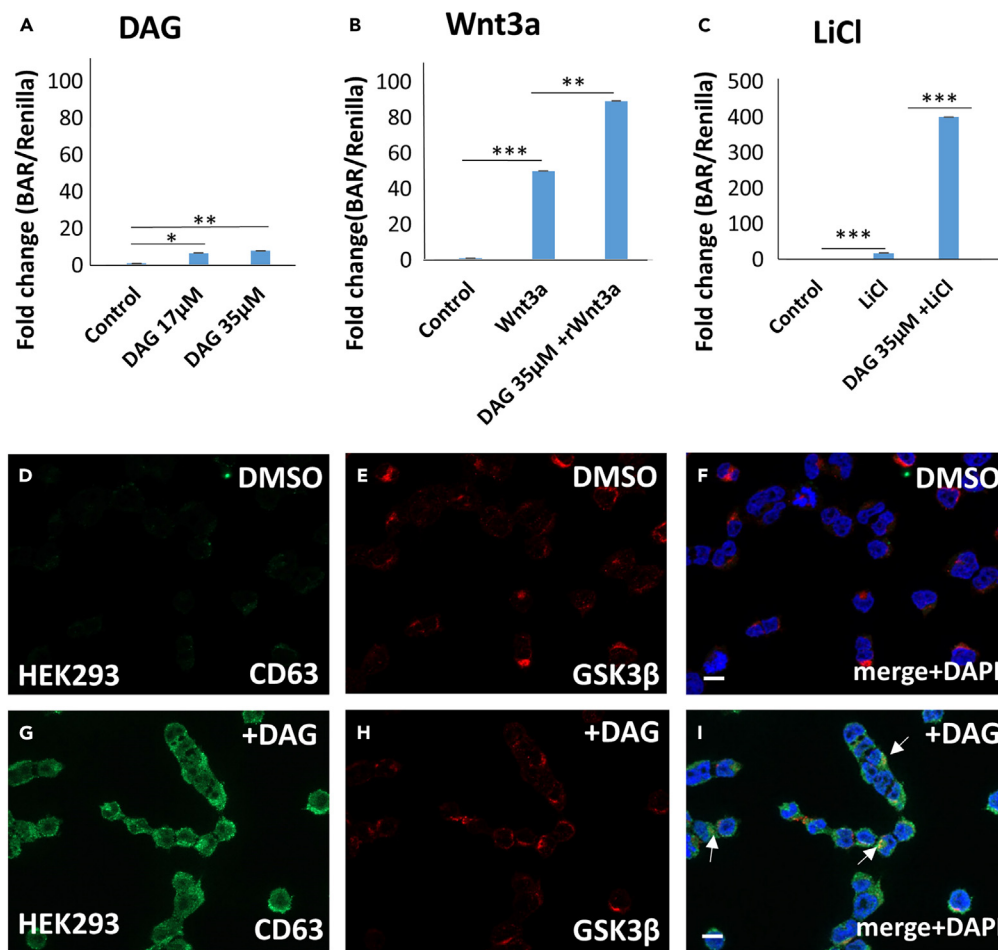


**Figure 3. DAG increases  $\beta$ -catenin activated reporter in HEK293 BAR/Renilla cells, and stabilizes MVB marker CD63**

(A) Exogenous DAG stimulated BAR-luciferase even in the absence of Wnt; this is probably due to the previously described weak background of endogenous Wnt signaling in this cell line.

(B) In the presence of recombinant Wnt3a, 35  $\mu$ M DAG stimulated the  $\beta$ -catenin transcriptional response.

(C) The response to LiCl, a GSK3 inhibitor that mimics Wnt signaling, was greatly increased by exogenous DAG. Each bar represents a biological triplicate.

(D) The MVB/lysosome marker CD63 was weakly stained in control HEK293 cells.

(E) GSK3 $\beta$  staining of HEK293 control cells.

(F) Merge with DAPI nuclear staining.

(G) CD63 staining was stabilized in HEK293 cells after 2 h DAG treatment.

(H) GSK3 $\beta$  staining in DAG treated HEK293 cells.

(I) Merge with DAPI showed that after DAG induction GSK3 $\beta$  is co-localized with CD63. Scale bars, 10  $\mu$ M; \* $p$  < 0.05, \*\* $p$  < 0.01 and \*\*\* $p$  < 0.001. Data are represented as mean  $\pm$  SD. See also Figure S1.

EIPA is considered the modern gold standard to diagnose macropinocytosis.<sup>34</sup> It has been previously shown that EIPA and the diuretic amiloride (which has been used in medical practice for 60 years), were able to inhibit macropinocytosis in SW480 cells.<sup>28</sup> The increase in nuclear  $\beta$ -catenin levels induced by DAG (compare Figures 5B–5D) were partially inhibited by the co-addition of EIPA (50  $\mu$ M) for 1 h (compare Figures 5D–5F). The increase in  $\beta$ -catenin by DAG and its inhibition by EIPA were confirmed by quantification using ImageJ (Figure 5G).

These experiments indicate that exogenous DAG, in addition to inducing macropinocytosis membrane activity, can increase nuclear  $\beta$ -catenin levels even in a CRC cell line in which Wnt signaling was previously thought to be fully activated by mutation of APC. This has implications for tumor progression. Given that DAG stimulates macropinocytosis and EIPA partially inhibits the DAG effect, the increase in  $\beta$ -catenin caused by DAG addition is likely driven by increased MVB trafficking.

### DAG microinjection mimics Wnt/ $\beta$ -catenin signaling in *Xenopus* embryos

To validate *in vivo* the crosstalk between DAG and  $\beta$ -catenin signaling, we turned to the *Xenopus laevis* embryo, a model system for the analysis of the Wnt signaling pathway. Microinjection of small amounts of LiCl (4 nL at 300 mM) into a ventral blastomere (Figure 6A) induces



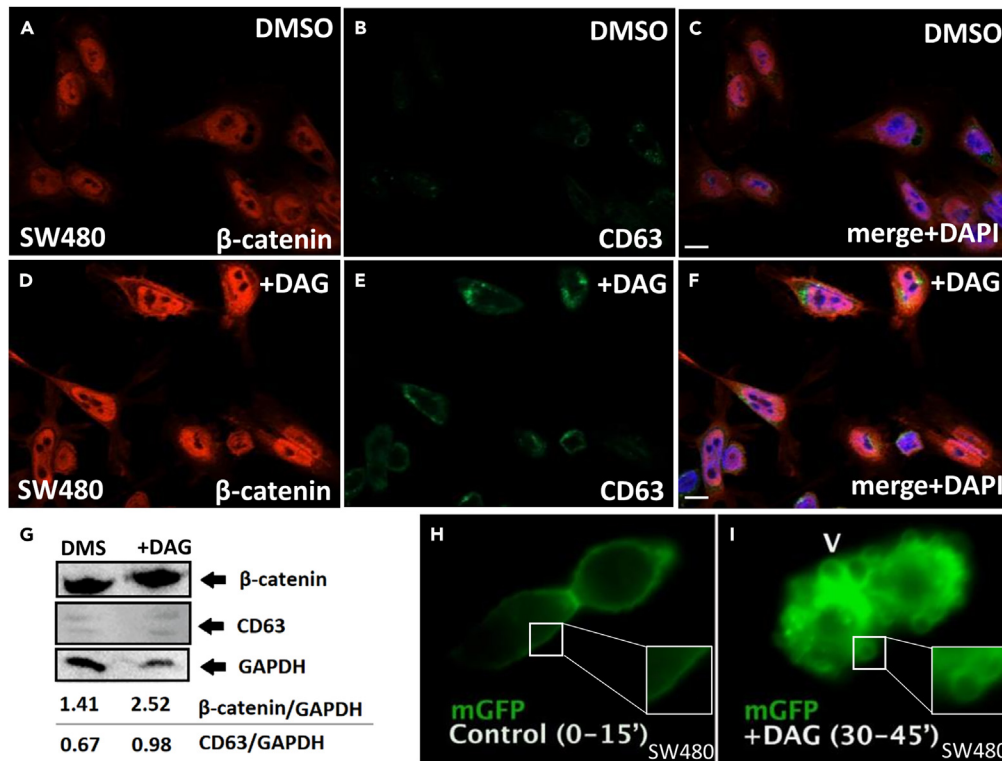


**Figure 4. Addition of DAG rapidly increases macropinosome-like vesicles in the plasma membrane, and elevates levels of nuclear  $\beta$ -catenin and of the MVB marker CD63 in SW480 CRC cells**

(A) Total  $\beta$ -catenin staining of SW480 control cells treated with DMSO.

(B) CD63 staining of same cells.

(C) Merge with DAPI staining.

(D) The addition of DAG (35  $\mu$ M dissolved in DMSO) to the culture medium increased nuclear  $\beta$ -catenin levels within 1 h in these cancer cells.

(E) The MVB/lysosome marker CD63 was also elevated by DAG addition, presumably as a consequence of increased macropinosocytosis.

(F) Merge with DAPI DNA staining confirming the increase in nuclear  $\beta$ -catenin induced by DAG. Scale bars, 10  $\mu$ M.

(G) Western blot of SW480 cells treated with DMSO alone or 35  $\mu$ M DAG in DMSO for 1 h. GAPDH was used as a loading control, note that the ratios of  $\beta$ -catenin and CD63 to GAPDH are increased by exogenous DAG.

(H and I) Transfected membrane-GFP demarcating the plasma membrane of two SW480 cells. DAG treatment strongly increased macropinosocytic-like vesicle membrane activity (arrowhead and inset) in the plasma membrane. These are still images from a 15 min movie shown in [Video S1](#). See also [Video S2](#) showing that the increase in macropinosocytosis occurs within the first few minutes of DAG addition. See also [Videos S1](#) and [S2](#).

dorsalization of embryos through the inhibition of GSK3, which manifests itself through enlarged head structures.<sup>42</sup> Co-injection with LiCl provides a sensitized assay system that has proven informative in previous studies.<sup>37</sup> As shown in [Figures 6B–6D](#), while LiCl alone only caused expanded head structures, co-injection of 3 mM DAG together with LiCl induced Wnt-like secondary axes, indicating a higher level of dorsalization activity. *In situ* hybridization with the pan-neural marker SOX2 confirmed that LiCl injection increased endogenous neural tissue, while partial ectopic neural axes lacking complete heads were induced only in combination with DAG. We conclude that microinjected DAG synergized with LiCl to activate the Wnt/ $\beta$ -catenin pathway *in vivo*.

## DISCUSSION

This investigation was prompted by two independent lines of evidence from separate laboratories. First, lipidomic studies in HCC cell lines showed that Wnt3a signaling was associated with a decrease in 1-palmitoyl-2-oleoyl-*sn*-glycerol (DG 16:0-18:1) in the plasma membrane, designated as DAG in this study.<sup>30</sup> Second, the emerging realization that macropinosocytosis, followed by MVB formation and lysosome acidification, is an essential part of canonical Wnt signaling.<sup>28</sup> This led us to formulate the working hypothesis that DAG might increase Wnt signaling through its function in macropinosocytic cup formation as outlined in [Figure 1A](#). Here, we provided evidence that exogenous *sn*-1,2 DAG added to the culture medium was able to significantly stimulate macropinosocytosis activity in the plasma membrane, expand the MVB compartment, and increase Wnt/ $\beta$ -catenin transcriptional signaling. DAG increased  $\beta$ -catenin levels in cancer cells mutant for APC, in which one could have presumed the  $\beta$ -catenin was fully stabilized already. This suggests that macropinosocytosis activation may aggravate tumor progression in Wnt-driven cancers.

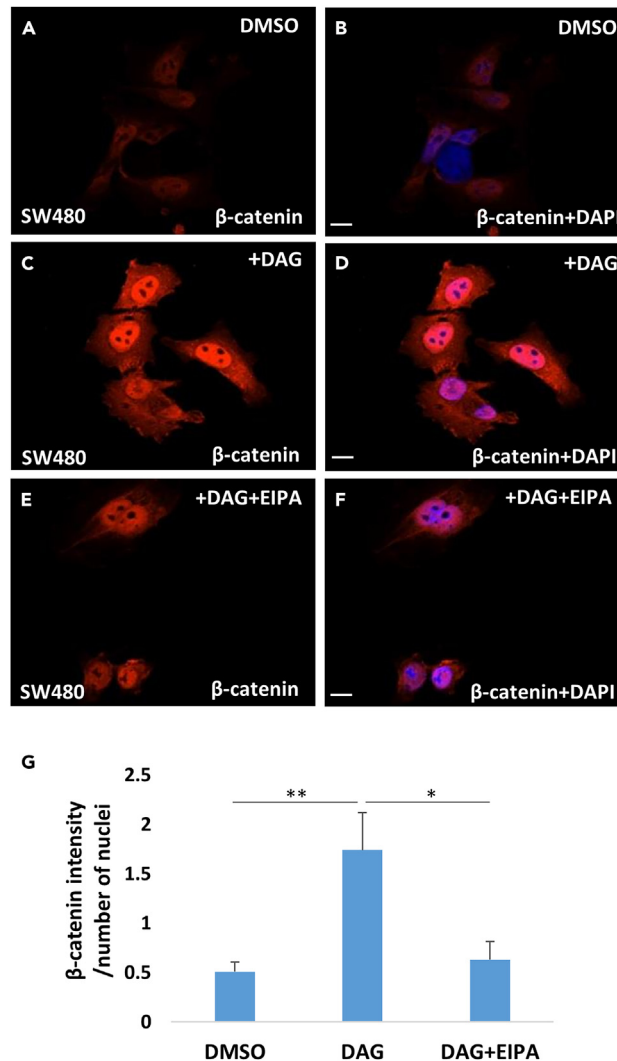


**Figure 5. The macropinocytosis inhibitor EIPA reduces nuclear  $\beta$ -catenin levels induced by DAG**

(A and B) Control SW480 cells were treated with DMSO (3%) for 1 h and counterstained with DAPI.

(C and D) The addition of DAG in the culture medium strongly increased  $\beta$ -catenin levels in SW480 cells in which Wnt/ $\beta$ -catenin is constitutively activated due to APC mutation.

(E and F) The addition of EIPA (50  $\mu$ M) partially reduced  $\beta$ -catenin levels, as can be noted in the decreased  $\beta$ -catenin/DAPI ratio in the merged images. Similar results were obtained in two independent experiments. Scale bars, 10  $\mu$ M.

(G) Quantification of the increase of  $\beta$ -catenin levels by DAG and its inhibition by EIPA. \* $p < 0.05$ , \*\* $p < 0.01$  and \*\*\* $p < 0.001$ . Data are represented as mean  $\pm$  SD.

DAG is found abundantly in our diet, where it is present in vegetable oils which consist of triacylglycerol (TAG) and DAG. For example, the highly beneficial olive oil contains 5.5% DAG.<sup>43</sup> There are 3 different isomers of DAG: sn-1,3; sn-2,3; and sn-1,2. Of these, only the sn-1,2 DAG enantiomer is capable of activating the PKC signaling pathway.<sup>3</sup> It is known that sn-1,3 DAG promotes weight loss in humans when compared to TAG oils.<sup>44</sup> Monoacylglycerol (MAG), TAG and free fatty acids are totally inactive on PKC.<sup>9</sup> The length of the fatty acid chain is important, with short fatty acids unable to stimulate PKC enzymatic activity.<sup>31</sup> In this study, we specifically used sn-1-palmitoyl-2-oleoyl-glycerol (DG 16:0-18:1, with the oleoyl chain having one unsaturated bond) which was identified by plasma membrane lipidomics.<sup>30</sup> Our observation that sn-1,2 DAG can increase  $\beta$ -catenin signals in cells mutant for APC when added to the culture medium suggests that diet lipids could play a role in the oncogenic progression of benign polyps in familial adenomatous polyposis.<sup>15</sup>

The tumor promoter PMA has been proposed to mimic the endogenous DAG second messenger signal. Repeated PMA treatment provides the classical tumor promoter paradigm in which cancer development can be accelerated by inflammatory agents without additional mutagenesis of DNA.<sup>5-7</sup> In a separate study, we provide evidence that PMA increases Wnt signaling, which can be blocked by inhibitors of macropinocytosis, MVB formation, membrane trafficking, and lysosome acidification.<sup>40</sup> Here, we showed that addition of DAG strongly

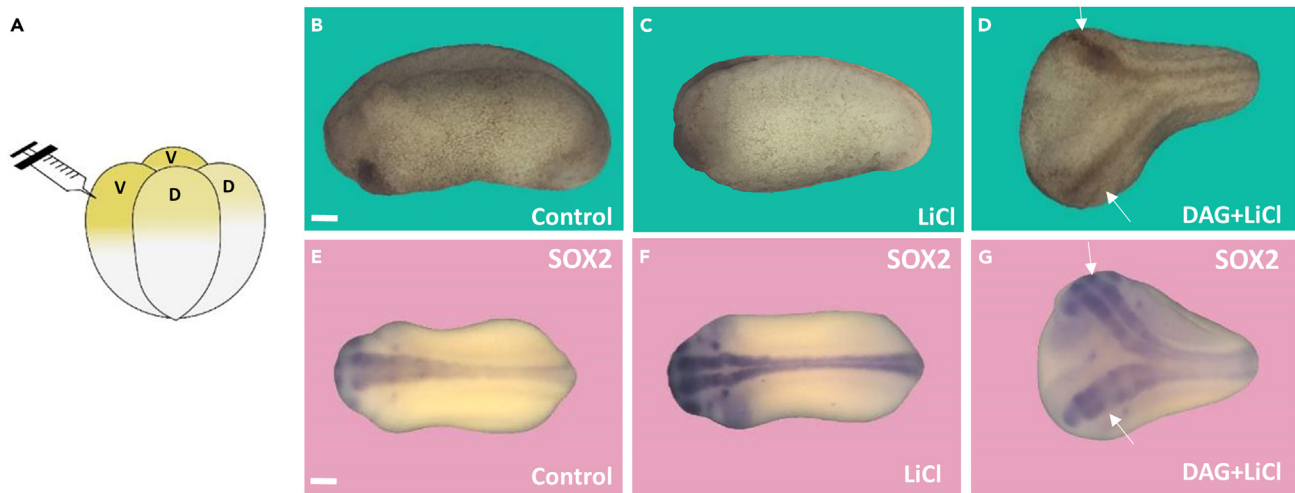


**Figure 6. DAG microinjection into *Xenopus* embryos causes the development of twinned axes in collaboration with the Wnt-mimic LiCl**

(A) Experimental design, a single 4 nL injection into a ventral blastomere at 4 cell stage.

(B) Uninjected control sibling at early tailbud (n = 33).

(C) LiCl injection (300 mM) causes weak dorsalization indicated by expanded anterior structures (n = 27, 100% with enlarged head phenotype).

(D) DAG (3 mM) together with LiCl induces the formation of partial double axes of the type caused by Wnt signaling (double axes in 62.3% of the embryos, n = 130, three experiments). Arrows show the first and secondary axes. Injection of DAG without LiCl had no effect (n = 37).

(E) *In situ* hybridization with the pan-neural SOX2 marker in control embryos.

(F) In LiCl microinjected embryos SOX2 neural staining was stronger, but only single axes were observed.

(G) SOX2 staining in embryos co-injected with DAG and LiCl showing two neural axes (arrows); this indicates a higher level of Wnt signaling *in vivo*. Scale bar, 200  $\mu$ M.

potentiates macropinocytosis and Wnt signaling. These findings have potential implications for the prevention of cancer progression. Pharmacological interventions targeting macropinocytosis, the  $\text{Na}^+/\text{H}^+$  exchanger (for example using the diuretic amiloride), multivesicular body formation, or reducing DAG levels, could slow tumor progression. Similarly, lysosomal activity, which is required for Wnt signaling, could be attenuated with inhibitors of Vacuolar-ATPase (V-ATPase) such as Bafilomycin, or lysosomotropic agents that alkalinize lysosomes.<sup>45</sup> Such therapies would have to be used in combination, and although they have not been successful yet, the results presented here suggest points of vulnerability for Wnt-driven cancer cells. DAG addition has not been extensively studied in the literature with a few exceptions.<sup>30,31</sup> However, the present study shows that DAG can have potent effects on Wnt/ $\beta$ -catenin signaling and macropinocytosis.

### Limitations of the study

Our study on the effect of DAG on macropinocytosis and Wnt signaling focused on the role of DAG in macropinosome formation.<sup>26,33</sup> However, DAG is a second messenger that participates in a myriad of biological processes. In addition to activating PKCs, DAG activates the Ras pathway through Ras guanyl nucleotide-releasing proteins (RasGRPs).<sup>46</sup> Many mutations in enzymes that regulate DAG are associated with cancer.<sup>3</sup> Therefore, what we present here is likely an oversimplification.

### STAR★METHODS

Detailed methods are provided in the online version of this paper and include the following:

- KEY RESOURCES TABLE
- RESOURCE AVAILABILITY
  - Lead contact
  - Materials availability
  - Data and code availability
- EXPERIMENTAL MODEL AND STUDY PARTICIPANT DETAILS
  - Cell culture and transfection
  - Immunofluorescence staining
  - *Xenopus* embryo microinjection and *in situ* hybridization
- METHOD DETAILS
  - TMR-dextran assay
  - Luciferase assay



- Western blots
- Time lapse imaging
- **QUANTIFICATION AND STATISTICAL ANALYSIS**
- Luciferase assay quantification
- Image quantification

## SUPPLEMENTAL INFORMATION

Supplemental information can be found online at <https://doi.org/10.1016/j.isci.2023.108075>.

## ACKNOWLEDGMENTS

This work was supported by the Norman Sprague Endowment for Molecular Oncology. GO has been supported by the bilateral grant of the British Council and the Scientific and Technological Research Council of Türkiye (TUBITAK grant number 217Z141) and the EMBO Installation Grant (IG 3024).

## AUTHOR CONTRIBUTIONS

Y.A. and E.D.R. designed the experiments and wrote the manuscript. Y.A., N.T.M., J.M., A.D., G.B., G.O., and E.D.R. performed experiments and contributed to the discussions.

## DECLARATION OF INTERESTS

The authors declare no competing interests.

Received: June 16, 2023

Revised: August 22, 2023

Accepted: September 25, 2023

Published: September 28, 2023

## REFERENCES

1. Czech, M.P. (2000). PIP2 and PIP3: complex roles at the cell surface. *Cell* 100, 603–606. [https://doi.org/10.1016/s0092-8674\(00\)80696-0](https://doi.org/10.1016/s0092-8674(00)80696-0).
2. Ueda, Y., Ishitsuka, R., Hüllin-Matsuda, F., and Kobayashi, T. (2014). Regulation of the transbilayer movement of diacylglycerol in the plasma membrane. *Biochimie* 107, 43–50. <https://doi.org/10.1016/j.biochi.2014.09.014>.
3. Cooke, M., and Kazanietz, M.G. (2022). Overarching roles of diacylglycerol signaling in cancer development and antitumor immunity. *Sci. Signal.* 15, eabo0264. <https://doi.org/10.1126/scisignal.abo0264>.
4. Clevers, H., and Nusse, R. (2012). Wnt/ $\beta$ -catenin signaling and disease. *Cell* 149, 1192–1205. <https://doi.org/10.1016/j.cell.2012.05.012>.
5. Berenblum, I. (1941). The cocarcinogenic action of croton resin. *Cancer Res.* 1, 44–48.
6. Rous, P., and Kidd, J.G. (1941). Conditional neoplasms and subthreshold neoplastic states: a study of the tar tumors of rabbits. *J. Exp. Med.* 73, 365–390. <https://doi.org/10.1084/jem.73.3.365>.
7. Weinberg, R.A. (2007). *The Biology of Cancer* (Garland Science), pp. 435–461.
8. Takai, Y., Kishimoto, A., Iwasa, Y., Kawahara, Y., Mori, T., and Nishizuka, Y. (1979). Calcium-dependent activation of a multifunctional protein kinase by membrane phospholipids. *J. Biol. Chem.* 254, 3692–3695. [https://doi.org/10.1016/S0021-9258\(18\)50638-4](https://doi.org/10.1016/S0021-9258(18)50638-4).
9. Nishizuka, Y. (1984). The role of protein kinase C in cell surface signal transduction and tumour promotion. *Nature* 308, 693–698. <https://doi.org/10.1038/308693a0>.
10. Newton, A.C. (2004). Diacylglycerol's affair with protein kinase C turns 25. *Trends Pharm. Sci.* 25, 175–177. <https://doi.org/10.1016/j.tips.2004.02.010>.
11. MacDonald, B.T., Tamai, K., and He, X. (2009). Wnt/ $\beta$ -catenin signaling: components, mechanisms, and diseases. *Dev. Cell* 17, 9–26. <https://doi.org/10.1016/j.devcel.2009.06.016>.
12. Niehrs, C. (2012). The complex world of WNT receptor signalling. *Nat. Rev. Mol. Cell Biol.* 13, 767–779. <https://doi.org/10.1038/nrm3470>.
13. Nusse, R., and Clevers, H. (2017). Wnt/ $\beta$ -catenin signaling, disease, and emerging therapeutic modalities. *Cell* 169, 985–999. <https://doi.org/10.1016/j.cell.2017.05.016>.
14. Galluzzi, L., Spranger, S., Fuchs, E., and López-Soto, A. (2019). WNT signaling in cancer immunosurveillance. *Trends Cell Biol.* 29, 44–65. <https://doi.org/10.1016/j.tcb.2018.08.005>.
15. Kinzler, K.W., and Vogelstein, B. (1996). Lessons from hereditary colorectal cancer. *Cell* 87, 159–170. [https://doi.org/10.1016/s0092-8674\(00\)81333-1](https://doi.org/10.1016/s0092-8674(00)81333-1).
16. Segditsas, S., and Tomlinson, I. (2006). Colorectal cancer and genetic alterations in the Wnt pathway. *Oncogene* 25, 7531–7537. <https://doi.org/10.1038/sj.onc.1210059>.
17. Khalaf, A.M., Fuentes, D., Morshid, A.I., Burke, M.R., Kaseb, A.O., Hassan, M., Hazle, J.D., and Elsayes, K.M. (2018). Role of Wnt/ $\beta$ -catenin signaling in hepatocellular carcinoma, pathogenesis, and clinical significance. *J. Hepat. Carcin.* 5, 61–73. <https://doi.org/10.2147/JHC.S156701>.
18. Waisberg, J., and Saba, G.T. (2015). Wnt/ $\beta$ -catenin pathway signaling in human hepatocellular carcinoma. *World J. Hepatol.* 7, 2631–2635. <https://doi.org/10.4254/wjh.v7.i26.2631>.
19. Taelman, V.F., Dobrowolski, R., Plouhinec, J.L., Fuentealba, L.C., Vorwald, P.P., Gumper, I., Sabatini, D.D., and De Robertis, E.M. (2010). Wnt signaling requires sequestration of glycogen synthase kinase 3 inside multivesicular endosomes. *Cell* 143, 1136–1148. <https://doi.org/10.1016/j.cell.2010.11.034>.
20. Albrecht, L.V., Tejeda-Muñoz, N., and De Robertis, E.M. (2021). Cell biology of canonical Wnt signaling. *Annu. Rev. Cell Dev. Biol.* 37, 369–389. <https://doi.org/10.1146/annurev-cellbio-120319-023657>.
21. Lewis, W.H. (1931). Pinocytosis. *Bull. John Hopkins Hosp.* 49, 17–27.
22. Bar-Sagi, D., and Feramisco, J.R. (1986). Induction of membrane ruffling and fluid-phase pinocytosis in quiescent fibroblasts by ras proteins. *Science* 233, 1061–1068. <https://doi.org/10.1126/science.3090687>.
23. Lambies, G., and Commisso, C. (2022). Macropinocytosis and cancer: From tumor stress to signaling pathways. *Subcell. Biochem.* 98, 15–40. [https://doi.org/10.1007/978-3-030-94004-1\\_2](https://doi.org/10.1007/978-3-030-94004-1_2).
24. Haigler, H.T., McKanna, J.A., and Cohen, S. (1979). Rapid stimulation of pinocytosis in human carcinoma cells A-431 by epidermal growth factor. *J. Cell Biol.* 83, 82–90. <https://doi.org/10.1083/jcb.83.1.82>.
25. Araki, N., Johnson, M.T., and Swanson, J.A. (1996). A role for phosphoinositide 3-kinase in the completion of macropinocytosis and

- phagocytosis by macrophages. *J. Cell Biol.* 135, 1249–1260. <https://doi.org/10.1083/jcb.135.5.1249>.
26. Yoshida, S., Pacitto, R., Inoki, K., and Swanson, J. (2018). Macropinocytosis, mTORC1 and cellular growth control. *Cell. Mol. Life Sci.* 75, 1227–1239. <https://doi.org/10.1007/s00018-017-2710-y>.
  27. Redelman-Sidi, G., Binyamin, A., Gaeta, I., Palm, W., Thompson, C.B., Romesser, P.B., Lowe, S.W., Bagul, M., Doench, J.G., Root, D.E., and Glickman, M.S. (2018). The canonical Wnt pathway drives macropinocytosis in cancer. *Cancer Res.* 78, 4658–4670. <https://doi.org/10.1158/0008-5472.CAN-17-3199>.
  28. Tejada-Muñoz, N., Albrecht, L.V., Bui, M.H., and De Robertis, E.M. (2019). Wnt canonical pathway activates macropinocytosis and lysosomal degradation of extracellular proteins. *Proc. Natl. Acad. Sci. USA* 116, 10402–10411. <https://doi.org/10.1073/pnas.1903506116>.
  29. Albrecht, L.V., Tejada-Muñoz, N., Bui, M.H., Cicchetto, A.C., Di Biagio, D., Colozza, G., Schmid, E., Piccolo, S., Christofk, H.R., and De Robertis, E.M. (2020). GSK3 inhibits macropinocytosis and lysosomal activity through the Wnt destruction complex machinery. *Cell Rep.* 32, 107973. <https://doi.org/10.1016/j.celrep.2020.107973>.
  30. Azbazar, Y., Demirci, Y., Heger, G., Ipekçil, D., Karabici, M., and Ozhan, G. (2023). Comparative membrane lipidomics of hepatocellular carcinoma cells reveals diacylglycerol and ceramide as key regulators of Wnt/ $\beta$ -catenin signaling and tumor growth. *Mol. Oncol.*
  31. Lapetina, E.G., Reep, B., Ganong, B.R., and Bell, R.M. (1985). Exogenous sn-1, 2-diacylglycerols containing saturated fatty acids function as bioregulators of protein kinase C in human platelets. *J. Biol. Chem.* 260, 1358–1361. [https://doi.org/10.1016/S0021-9258\(18\)89595-3](https://doi.org/10.1016/S0021-9258(18)89595-3).
  32. Swanson, J.A. (2008). Shaping cups into phagosomes and macropinosomes. *Nat. Rev. Mol. Cell Biol.* 9, 639–649. <https://doi.org/10.1038/nrm2447>.
  33. Swanson, J.A. (1989). Phorbol esters stimulate macropinocytosis and solute flow through macrophages. *J. Cell Sci.* 94, 135–142. <https://doi.org/10.1242/jcs.94.1.135>.
  34. Commisso, C., Davidson, S.M., Soydaner-Azeloglu, R.G., Parker, S.J., Kamphorst, J.J., Hackett, S., Grabocka, E., Nofal, M., Drebin, J.A., Thompson, C.B., et al. (2013). Macropinocytosis of protein is an amino acid supply route in Ras-transformed cells. *Nature* 497, 633–637. <https://doi.org/10.1038/nature12138>.
  35. Biechele, T.L., and Moon, R.T. (2008). Assaying  $\beta$ -catenin/TCF transcription with  $\beta$ -catenin/TCF transcription-based reporter constructs. *Methods Mol. Biol.* 468, 99–110. [https://doi.org/10.1007/978-1-59745-249-6\\_8](https://doi.org/10.1007/978-1-59745-249-6_8).
  36. Colozza, G., Jami-Alahmadi, Y., Dsouza, A., Tejada-Muñoz, N., Albrecht, L.V., Sosa, E.A., Wohlschlegel, J.A., and De Robertis, E.M. (2020). Wnt-inducible Lrp6-APEX2 interacting proteins identify ESCRT machinery and Trk-fused gene as components of the Wnt signaling pathway. *Sci. Rep.* 10, 21555. <https://doi.org/10.1038/s41598-020-78019-5>.
  37. Tejada-Muñoz, N., and De Robertis, E.M. (2022). Lysosomes are required for early dorsal signaling in the *Xenopus* embryo. *Proc. Natl. Acad. Sci. USA* 119, e2201008119. <https://doi.org/10.1073/pnas.2201008119>.
  38. Leibovitz, A., Stinson, J.C., McCombs, W.B., III, McCoy, C.E., Mazur, K.C., and Mabry, N.D. (1976). Classification of human colorectal adenocarcinoma cell lines. *Cancer Res.* 36, 4562–4569.
  39. Faux, M.C., Ross, J.L., Meeker, C., Johns, T., Ji, H., Simpson, R.J., Layton, M.J., and Burgess, A.W. (2004). Restoration of full-length adenomatous polyposis coli (APC) protein in a colon cancer cell line enhances cell adhesion. *J. Cell Sci.* 117, 427–439. <https://doi.org/10.1242/jcs.00862>.
  40. Tejada Munoz, N., Azbazar, Y., Monka, J., Binder, G., Ayala, R., Dayrit, A., O'Brien, N., and De Robertis, E.M. (2023). The PMA Phorbol Ester Tumor Promoter Increases Canonical Wnt Signaling via Macropinocytosis. Preprint at bioRxiv. <https://doi.org/10.1101/2023.06.02.543509>.
  41. Koivusalo, M., Welch, C., Hayashi, H., Scott, C.C., Kim, M., Alexander, T., Touret, N., Hahn, K.M., and Grinstein, S. (2010). Amiloride inhibits macropinocytosis by lowering submembranous pH and preventing Rac1 and Cdc42 signaling. *J. Cell Biol.* 188, 547–563. <https://doi.org/10.1083/jcb.200908086>.
  42. Kao, K.R., Masui, Y., and Elinson, R.P. (1986). Lithium-induced respecification of pattern in *Xenopus laevis* embryos. *Nature* 322, 371–373. <https://doi.org/10.1038/322371a0>.
  43. Lee, W.J., Zhang, Z., Lai, O.M., Tan, C.P., and Wang, Y. (2020). Diacylglycerol in food industry: Synthesis methods, functionalities, health benefits, potential risks and drawbacks. *Trends Food Sci. Tech.* 97, 114–125. <https://doi.org/10.1016/j.tifs.2019.12.032>.
  44. Maki, K.C., Davidson, M.H., Tsushima, R., Matsuo, N., Tokimitsu, I., Umporowicz, D.M., Dicklin, M.R., Foster, G.S., Ingram, K.A., Anderson, B.D., et al. (2002). Consumption of diacylglycerol oil as part of a reduced-energy diet enhances loss of body weight and fat in comparison with consumption of a triacylglycerol control oil. *Am. J. Clin. Nutr.* 76, 1230–1236. <https://doi.org/10.1093/ajcn/76.6.1230>.
  45. Rebecca, V.W., Nicastrì, M.C., McLaughlin, N., Fennelly, C., McAfee, Q., Ronghe, A., Nofal, M., Lim, C.Y., Witze, E., Chude, C.I., et al. (2017). A unified approach to targeting the lysosome's degradative and growth signaling roles: dimeric quinacrine identifies new lysosomal target in cancer. *Cancer Discov.* 7, 1266–1283. <https://doi.org/10.1158/2159-8290.CD-17-0741>.
  46. Griner, E.M., and Kazanietz, M.G. (2007). Protein kinase C and other diacylglycerol effectors in cancer. *Nat. Rev. Cancer* 7, 281–294. <https://doi.org/10.1038/nrc2110>.

## STAR★METHODS

### KEY RESOURCES TABLE

REAGENT or RESOURCE	SOURCE	IDENTIFIER
<b>Antibodies</b>		
rabbit anti- $\beta$ catenin	Invitrogen	Cat# 71-2700; RRID: AB_2533982
mouse anti-CD63	Santa Cruz	Cat# sc5275; RRID: AB_627877
Goat anti-mouse IgG Alexa Fluor 488	Invitrogen	Cat # A-11001; RRID: AB_2534069
Goat anti-rabbit-Alexa Fluor 594	Invitrogen	Cat # A-11012; RRID: AB_2534079
<b>Chemicals, peptides, and recombinant proteins</b>		
Wnt3a	Peptotech	Cat# 315-20
Lipofectamine 3000	ThermoFisher	Cat# L3000001
Lithium chloride (LiCl)	Sigma	Cat# L4408
Dextran Tetramethylrhodamine (TMR-Dx) 70,000	ThermoFisher	Cat# D1818
1-palmitoyl-2-oleoyl-sn-glycerol (DG 16:0-18:1)	Avanti Polar Lipids	Cat# 800815O
5-(N-Ethyl-N-isopropyl) amiloride (EIPA)	Sigma	Cat# A3085
Dulbecco's Modified Eagle Medium (DMEM)	Gibco	Cat# 11965092
Fetal Bovine Serum (FBS)	ThermoFisher	Cat#16000044
Pen-Strep antibiotics	ThermoFisher	Cat#15140122
Glutamine	ThermoFisher	Cat#25030081
Circular coverslips	ibidi	Cat#10815
8-well glass-bottom chamber slides	ibidi	Cat#80827
12-well dish	ThermoFisher	Cat#150628
10-cm dish	ThermoFisher	Cat#174903
PBS	Fisher	Cat# BP339
Bovine Serum Albumin (BSA)	ThermoFisher	Cat#9048468
Fluoro-shield Mounting Medium with DAPI	Abcam	Cat# ab104139
Paraformaldehyde	Sigma	Cat#P6148
Fluoroshield Mounting Medium with DAPI	Abcam	Cat# ab104139
<b>Critical commercial assays</b>		
Dual-Luciferase Reporter Assay System	Promega	Cat# E1500
<b>Experimental models: Cell lines</b>		
SW480	ATCC	RRID:CVCL_0546
<b>Experimental models: Organisms/strains</b>		
Xenopus laevis	Nasco	N/A
<b>Recombinant DNA</b>		
pCS2-mGFP	Addgene	RRID:Addgene_14757
b-catenin Activated Reporter (BAR)	Addgene	RRID:Addgene_12456
Renilla reporter	Addgene	RRID:Addgene_6218
<b>Software and algorithms</b>		
ImageJ	NIH	<a href="https://imagej.nih.gov/ij/">https://imagej.nih.gov/ij/</a>
Zen 2.3 imaging software	Zeiss	<a href="http://www.zeiss.com">http://www.zeiss.com</a>
Axiovision 4.8	Zeiss	<a href="http://www.zeiss.com">http://www.zeiss.com</a>

(Continued on next page)

**Continued**

REAGENT or RESOURCE	SOURCE	IDENTIFIER
Other		
IM 300 microinjection pump	Narishige International USA, Inc	N/A
Axio Observer Z1 Inverted Microscope with Apotome	Zeiss	N/A
Zeiss Observer.Z1 microscope	Zeiss	N/A

**RESOURCE AVAILABILITY****Lead contact**

Further information and requests for resources and reagents should be directed to and will be fulfilled by the Lead Contact, Dr. Edward M. De Robertis ([Ederobertis@mednet.ucla.edu](mailto:Ederobertis@mednet.ucla.edu)).

**Materials availability**

No new unique reagents were generated.

**Data and code availability**

Data reported in this paper will be shared by the [lead contact](#) upon request.

No custom code, software, or algorithm central to supporting the main claims of the paper were generated in this manuscript.

**EXPERIMENTAL MODEL AND STUDY PARTICIPANT DETAILS****Cell culture and transfection**

HEK293 cells were cultured in high glucose DMEM (Dulbecco's Modified Eagle Medium-CAT:11965092, Gibco) supplemented with 10% FBS (fetal bovine serum) and SW480 cells were grown in RPMI 1640 (CAT:11875093, Gibco) medium with 10% FBS in a 5% CO<sub>2</sub> humidified environment at 37°C. Lipofectamine 3000 was used for transfection. Cells were seeded in a 12 well plate or chamber. 24h later, HEK293 cells were transfected with GSK3β.

**Immunofluorescence staining**

SW480 cells were seeded on cover glass in 24-well culture plates. Cells were treated with DAG (50 μM) for 1h with or without EIPA (50 μM) at 37°C for 1h. After incubation, cover glasses were removed, and cells washed with PBS. Then they were fixed with 4% PFA in PBS for 15 min. Next, cells were washed with PBS three times, 0.2% Tween-20 diluted in PBS for 10 min, and further washed with PBS two times. After that, cells were incubated with blocking buffer (1% BSA dissolved in PBS) for 1 h. After blocking, cells were incubated with the primary antibodies rabbit anti-β catenin (CAT:71-2700, Invitrogen, Massachusetts, USA), and anti-CD63, MVBs marker, (CAT:sc5275, Santa Cruz, Texas, USA) in PBS containing 1% for 1h. After incubation, cells were washed three times with PBS and next, incubated with the secondary antibodies Alexa Fluor 594 (1:200, ThermoFisher Scientific, MA, USA), and goat anti-mouse IgG Alexa Fluor 488 (1:200, ThermoFisher Scientific, MA, USA) for 1 hour at room temperature (RT). After that, cells were washed with PBS three times and were mounted using mounting medium including 4',6-diamidino-2-phenylindole (DAPI, 0.5 ug/ml, 4083S, Cell Signaling Technology, MA, USA). Immunostainings were imaged with a Carl Zeiss Axio Observer Z1 Inverted Microscope with Apotome.

**Xenopus embryo microinjection and *in situ* hybridization**

*Xenopus laevis* embryos were generated by *in vitro* fertilization with dissected testes as described.<sup>37</sup> Ventral injection of 4 nL LiCl (300 mM) ± DAG (3 mM) was performed at the 4-8 cell stage. Embryos were fixed using 4% PFA at early tailbud (stage 22) and imaged using Carl Zeiss Axio Zoom.V16. *In situ* hybridizations were performed as described at <http://www.hhmi.ucla.edu/derobertis> using SOX2 probe.

**METHOD DETAILS****TMR-dextran assay**

HEK293 cells were seeded on cover glass coverslips overnight. Then cells were incubated with 1 mg/mL TMR for 1 h with or without DAG (35 μM) in an incubator with 5% CO<sub>2</sub> at 37°C. At the end of incubation, cells were washed 3 times for 5 minutes each with PBS (Fisher BP339, containing 157 mM Na<sup>+</sup>, 140 mM Cl<sup>-</sup>, 4.45mM K<sup>+</sup>, 10.1 mM HPO<sub>4</sub><sup>2-</sup>, 1.76 mM H<sub>2</sub>PO<sub>4</sub><sup>-</sup> at pH 7.4), and fixed using 4% paraformaldehyde (PFA) diluted in PBS. Coverslips were mounted using Fluoro-shield Mounting Medium with DAPI (ab104139) from Abcam. Results were photographed using a Zeiss Imager Z.1 microscope with Apotome.

### Luciferase assay

HEK293 BAR/Renilla reporter cells<sup>28</sup> were seeded on 24-well culture plates. After 24 h, cells were treated with DAG (17 or 35  $\mu$ M) with or without rWnt3a (100 ng/mL) or LiCl (40 mM) overnight at 37°C. Reporter activity was measured using the luciferase reporter assay kit (Promega, WI, USA).

### Western blots

Cells were lysed using RIPA buffer (0.1% NP40, 10% Glycerol, 20 mM Tris/HCl, pH 7.5) containing phosphatase inhibitors (Calbiochem #524629) and protease inhibitors (Roche #04693132001).

### Time lapse imaging

SW480 cells were seeded on the optics of glass in a petri and on the 2<sup>nd</sup> day, they were transfected with membrane-GFP<sup>29</sup> using Lipofectamine 3000. 3 days later, cells were filmed and then treated with DAG (125  $\mu$ M) for 30 min. Videos were taken using Zeiss Observer.Z1 microscope and AxioVision 4.8.2 SP3 software.

## QUANTIFICATION AND STATISTICAL ANALYSIS

### Luciferase assay quantification

Statistical analysis for Luciferase assays was carried out using Student's t-test. \*\*\*p < 0.001, \*\*p < 0.01, and \*p < 0.05; error bars represent standard deviation (SD).

### Image quantification

The data are performed as means and standard deviations (SD) and as a statistical analysis the Student's t-test was used. p value of <0.05 was considered statistically significant. The intensity of vesicles in the immunofluorescence was calculated from the red channel using the ImageJ software and a computer-assisted particle analysis tool and it was divided number of nuclei in each microscope field, using n > 25 per condition. The Graphical Abstract was made using BioRender.